J. Inst. Math. Jussieu (2022), 1–21
doi:10.1017/S1474748021000591

GENUS 1 MINIMAL k-NOIDS AND SADDLE TOWERS IN $\mathbb{H}^2 \times \mathbb{R}$

JESÚS CASTRO-INFANTES[1] AND JOSÉ M. MANZANO[2]

[1]*Departamento de Geometría y Topología, Universidad de Granada, Avda. Fuentenueva s/n 18071 Granada, Spain*
(jcastroinfantes@ugr.es)

[2]*Departamento de Matemáticas, Universidad de Jaén, Campus Las Lagunillas s/n 23071 Jaén, Spain*
(jmprego@ujaen.es)

(Received 27 January 2020; revised 3 November 2021; accepted 7 November 2021)

Abstract For each $k \geq 3$, we construct a 1-parameter family of complete properly Alexandrov-embedded minimal surfaces in the Riemannian product space $\mathbb{H}^2 \times \mathbb{R}$ with genus 1 and k embedded ends asymptotic to vertical planes. We also obtain complete minimal surfaces with genus 1 and $2k$ ends in the quotient of $\mathbb{H}^2 \times \mathbb{R}$ by an arbitrary vertical translation. They all have dihedral symmetry with respect to k vertical planes, as well as finite total curvature $-4k\pi$. Finally, we provide examples of complete properly Alexandrov-embedded minimal surfaces with finite total curvature with genus 1 in quotients of $\mathbb{H}^2 \times \mathbb{R}$ by the action of a hyperbolic or parabolic translation.

Key words and phrases: minimal surfaces, finite total curvature, minimal k-noids, saddle towers, conjugate construction

2020 Mathematics Subject Classification: Primary 53A10
Secondary 53C30

1. Introduction

The theory of complete minimal surfaces in $\mathbb{H}^2 \times \mathbb{R}$ with finite total curvature – that is, those whose Gauss curvature is integrable – has received considerable attention during the last decade, mainly triggered by Collin and Rosenberg [2]. The combined work of Hauswirth, Nelli, Sa Earp, and Toubiana [6], and Hauswirth, Menezes, and Rodríguez [5] shows that a complete minimal surface immersed in $\mathbb{H}^2 \times \mathbb{R}$ has finite total curvature if and only if it is proper, has finite topology, and has each of its ends asymptotic to an admissible polygon – that is, a curve homeomorphic to $\mathbb{S}^1$ consisting of finitely many alternating complete vertical and horizontal ideal geodesics (see [5]). Here the product compactification of $\mathbb{H}^2 \times \mathbb{R}$ is considered, in which the horizontal (resp., vertical) ideal boundary consists of two disks $\mathbb{H}^2 \times \{\pm\infty\}$ (resp., the cylinder $\partial_\infty \mathbb{H}^2 \times \mathbb{R}$). Ideal horizontal geodesics are those of the form $\Gamma \times \{+\infty\}$ or $\Gamma \times \{-\infty\}$, where Γ is a geodesic of $\mathbb{H}^2$, whereas ideal vertical geodesics are those of the form $\{p_\infty\} \times \mathbb{R}$, where $p_\infty \in \partial_\infty \mathbb{H}^2$ is an ideal point.

Combining this classification with the previous work of Hauswirth and Rosenberg [7], the following Gauss–Bonnet-type formula for a complete minimal surface Σ immersed in $\mathbb{H}^2\times\mathbb{R}$ with finite total curvature holds true:

$$\int_\Sigma K = 2\pi\chi(\Sigma) - 2\pi m = 2\pi(2-2g-k-m), \tag{1.1}$$

where g and k are, respectively, the genus and the number of ends of Σ, $\chi(\Sigma)=2-2g-k$ its Euler characteristic, K its Gauss curvature, and m the total number of horizontal ideal geodesics in $\mathbb{H}^2\times\{+\infty\}$, among all polygonal components associated with the ends of Σ. Observe that the union of all these components consists of m ideal horizontal geodesics in $\mathbb{H}^2\times\{+\infty\}$, m ideal horizontal geodesics in $\mathbb{H}^2\times\{-\infty\}$, and $2m$ ideal vertical geodesics, so the term $2\pi m$ in equation (1.1) can be understood as the sum of exterior angles of the asymptotic boundary of Σ. We also remark that equation (1.1) has been extended to some quotients of $\mathbb{H}^2\times\mathbb{R}$ by Hauswirth and Menezes [4].

Although this characterization is very satisfactory from a theoretical point of view, it seems tough in general to determine whether or not a given family of admissible polygons actually bounds a minimal surface, or if a given topological type can be realized by such a surface. In fact, there are not many examples of surfaces with finite total curvature in the literature. Let us highlight some of them in terms of the three parameters (g,k,m) appearing in equation (1.1):

- The simplest case is that of flat minimal surfaces, which must be vertical planes (i.e., of the form $\Gamma\times\mathbb{R}$, where $\Gamma\subset\mathbb{H}^2$ is a complete geodesic) because of the Gauss equation. In particular, vertical planes are the only complete minimal surfaces with finite total curvature and $(g,k,m)=(0,1,1)$ (see also [8, Corollary 5]).
- A minimal Scherk graph in $\mathbb{H}^2\times\mathbb{R}$ is a minimal graph over a geodesic ideal polygon of $\mathbb{H}^2$ with $2a$ vertices, $a\geq 2$, taking alternating limit values $+\infty$ and $-\infty$ on the sides of the polygon. A characterization of polygons carrying such a surface is analyzed in [14], in which case they have finite total curvature and satisfy $(g,k,m)=(0,1,a)$. The case $a=2$ gives rise to the only complete minimal surfaces with total curvature -2π, as shown by Pyo and Rodríguez [21, Theorem 4.1]. We can find as well the *twisted* Scherk minimal surfaces [21] with $(g,k,m)=(0,1,2b+1)$, $b\geq 1$, and total curvature $-4b\pi$ that are no longer graphs or bigraphs, some of which are embedded.
- Minimal k-noids constructed by Morabito and Rodríguez [16] (also by Pyo [20] in the symmetric case) have finite total curvature, genus 0, and k ends asymptotic to vertical planes. This gives $g=0$ and $k=m\geq 2$.
- Horizontal catenoids are the only complete minimal surfaces immersed in $\mathbb{H}^2\times\mathbb{R}$ with finite total curvature and $k=m=2$ (see [5, 6]). The family of minimal surfaces with finite total curvature and $k=m\geq 3$ is not hitherto well understood, not even in the case $g=0$. The most general construction was given by Martín, Mazzeo, and Rodríguez [12], who found properly embedded minimal surfaces with finite total curvature in $\mathbb{H}^2\times\mathbb{R}$ of genus g and k ends asymptotic to vertical planes (and hence $m=k$), for arbitrary $g\geq 0$ and k arbitrarily large depending on g.

In this paper we provide highly symmetric examples with $g = 1$ and $m = k \geq 3$, which are hence conformally equivalent to a torus with k punctures. They can be thought of as the counterpart in $\mathbb{H}^2 \times \mathbb{R}$ of the genus 1 minimal k-noids in $\mathbb{R}^3$ obtained by Mazet [13]. Outside a compact subset, our surfaces look like the minimal k-noids in [16, 20], and they are not globally embedded in general. Notice that there are no such examples with $k = 2$, due to the aforesaid uniqueness of horizontal catenoids in [6]. Our main result can be stated as follows:

Theorem 1. *For each $k \geq 3$, there exists a 1-parameter family of properly Alexandrov-embedded minimal surfaces in $\mathbb{H}^2 \times \mathbb{R}$ with genus 1 and k ends, dihedrally symmetric with respect to k vertical planes and symmetric with respect to a horizontal plane. They have finite total curvature $-4k\pi$, and each of their ends is embedded and asymptotic to a vertical plane.*

The construction of these genus 1 minimal k-noids is based on a conjugate technique, in the sense of Daniel [3] and Hauswirth, Sa Earp, and Toubiana [8]. Conjugation has been a fruitful technique to obtain constant-mean-curvature surfaces in $\mathbb{H}^2 \times \mathbb{R}$ and $\mathbb{S}^2 \times \mathbb{R}$ (see [10, 11, 9, 13, 15, 16, 19, 18, 20] and the references therein). We begin by considering a solution to an improper Dirichlet problem [14, 17] in $\mathbb{H}^2 \times \mathbb{R}$ over an unbounded geodesic triangle $\Delta \subset \mathbb{H}^2$, a so-called Jenkins–Serrin problem [14]. These solutions are minimal graphs over the interior of Δ with prescribed finite and infinite values when one approaches $\partial\Delta$. The conjugate surface is another minimal graph in $\mathbb{H}^2 \times \mathbb{R}$ whose boundary is made of curves lying on totally geodesic surfaces – that is, vertical and horizontal planes. Since there are isometric reflections across such planes in $\mathbb{H}^2 \times \mathbb{R}$, the conjugate surface can be extended to a complete surface under suitable conditions. In order to prescribe the symmetries stated in Theorem 1, we will encounter two period problems that will impose further restrictions on Δ and on the boundary values of the Jenkins–Serrin problem.

Our conjugate approach is inspired by the genus 1 minimal k-noids in $\mathbb{R}^3$ given by Mazet [13], and by the mean-curvature $\frac{1}{2}$ surfaces in $\mathbb{H}^2 \times \mathbb{R}$ given by Plehnert [19]. It is important to remark that there exist technical dissimilarities between the cases $H = 0$ and $H = \frac{1}{2}$ in $\mathbb{H}^2 \times \mathbb{R}$, because of the fact that the conjugate of a surface with mean curvature $\frac{1}{2}$ (resp., 0) is a minimal surface in the Heisenberg group Nil_3 (resp., $\mathbb{H}^2 \times \mathbb{R}$). Furthermore, our construction can be adapted to produce complete minimal surfaces that are invariant by an arbitrary vertical translation (i.e., in the direction of the factor $\mathbb{R}$), similar to the saddle towers given in [16]. They have genus 1 in the quotient and they are not embedded in general.

Theorem 2. *For each $k \geq 3$ and each vertical translation T, there is a 1-parameter family of Alexandrov-embedded singly periodic minimal surfaces in $\mathbb{H}^2 \times \mathbb{R}$ that are invariant by T and dihedrally symmetric with respect to k vertical planes and a horizontal plane. They have finite total curvature $-4k\pi$, genus 1, and $2k$ vertical ends in the quotient of $\mathbb{H}^2 \times \mathbb{R}$ by T.*

Our analysis of the period problems will allow us to find surfaces that are invariant not by a discrete group of rotations but by discrete groups of parabolic or hyperbolic

translations, which we will call *parabolic and hyperbolic* ∞*-noids*, respectively. These surfaces have infinitely many ends, and we can guarantee that many of the examples are properly embedded in the hyperbolic case. Although we will not state it explicitly, analogous surfaces can be obtained in the quotient of $\mathbb{H}^2\times\mathbb{R}$ by an arbitrary vertical translation in the spirit of Theorem 2, giving rise to doubly periodic examples in which the Hauswirth–Menezes formula [4] for finite-total-curvature surfaces applies in the quotient.

Theorem 3. *There is a* 2*-parameter (resp.,* 1*-parameter) family of properly embedded (resp., Alexandrov-embedded) minimal surfaces in* $\mathbb{H}^2\times\mathbb{R}$ *with genus* 0 *and infinitely many ends, invariant by a discrete group of hyperbolic (resp., parabolic) translations. Each of their ends is embedded and asymptotic to a vertical plane, and has finite total curvature.*

The paper is organized as follows: In §2 we will analyze some aspects of the conjugation of surfaces in $\mathbb{H}^2\times\mathbb{R}$ that will be needed in the construction, and §3 will be devoted to filling in the details of the proofs of Theorems 1 and 2. We will also discuss some open questions about the uniqueness and embeddedness of the constructed surfaces, as well as natural limits of the 1-parameter family of genus 1 k-noids. In the last part of the paper we will prove Theorem 3.

2. Preliminaries

Let Σ be a simply connected Riemannian surface. Given an isometric minimal immersion $X:\Sigma\to\mathbb{H}^2\times\mathbb{R}$, Hauswirth, Sa Earp, and Toubiana [8] proved the existence of another isometric minimal immersion $\widetilde{X}:\Sigma\to\mathbb{H}^2\times\mathbb{R}$ such that the following are true:

(1) Both immersions induce the same angle function $\nu=\langle N,\partial_t\rangle=\langle\widetilde{N},\partial_t\rangle$, where N and $\widetilde{N}$ stand for unit normal vector fields to X and $\widetilde{X}$, respectively, and ∂_t is the unit vector field in $\mathbb{H}^2\times\mathbb{R}$ in the direction of the factor $\mathbb{R}$.

(2) The shape operators S and $\widetilde{S}$ of X and $\widetilde{X}$, respectively, satisfy $\widetilde{S}=JS$, where J is the $\frac{\pi}{2}$-rotation in $T\Sigma$, chosen such that both $\{\mathrm{d}X_p(u),\mathrm{d}X_p(Ju),N_p\}$ and $\{\mathrm{d}\widetilde{X}_p(u),\mathrm{d}\widetilde{X}_p(Ju),\widetilde{N}_p\}$ are positively oriented bases in $\mathbb{H}^2\times\mathbb{R}$ for all nonzero tangent vectors $u\in T_p\Sigma$.

(3) The tangential components $T=\partial_t-\nu N$ and $\widetilde{T}=\partial_t-\nu\widetilde{N}$ of ∂_t satisfy $\widetilde{X}^*\widetilde{T}=JX^*T$. This implies that $\langle\mathrm{d}X_p(u),\partial_t\rangle=\langle\mathrm{d}\widetilde{X}_p(Ju),\partial_t\rangle$ for all $u\in T_p\Sigma$.

The immersions X and $\widetilde{X}$ are called *conjugate* and determine each other up to ambient isometries preserving both the global orientation and the vector field ∂_t. Our initial surface $X(\Sigma)$ will be a vertical graph over a convex domain, namely a solution of a Jenkins–Serrin problem. This implies that $\widetilde{X}(\Sigma)$ is also a vertical graph over another (possibly nonconvex) domain, due to the Krust-type theorem given by [8, Theorem 14]. Therefore, we can assume that both surfaces are embedded, and we will use the notation Σ and $\widetilde{\Sigma}$ for the surfaces $X(\Sigma)$ and $\widetilde{X}(\Sigma)$, respectively.

Although the conjugate surface $\widetilde{\Sigma}$ is not explicit in general, one can obtain insightful information if the initial surface Σ has boundary consisting of horizontal and vertical geodesics intersecting at some vertices. A curve $\Gamma\subset\Sigma$ is a horizontal (resp., vertical) geodesic in $\mathbb{H}^2\times\mathbb{R}$ if and only if the conjugate curve $\widetilde{\Gamma}\subset\widetilde{\Sigma}$ lies in a vertical (resp.,

horizontal) totally geodesic surface of $\mathbb{H}^2\times\mathbb{R}$ intersecting $\widetilde{\Sigma}$ orthogonally along $\widetilde{\Gamma}$. Furthermore, axial symmetry about Γ corresponds to mirror symmetry about $\widetilde{\Gamma}$, which enables analytic continuation of Σ and $\widetilde{\Sigma}$ across their boundaries. If the angles at the vertices of $\partial\Sigma$ are integer divisors of π, then no singularity appears at such vertices after successive reflections about the boundary components, and both surfaces can be extended to complete (possibly nonembedded) minimal surfaces. We refer to [10, 19, 15] for details.

However, most difficulties concerning the depiction of $\widetilde{\Sigma}$, and in particular deciding whether or not it is embedded, show up when one tries to understand the behavior of the conjugate of a vertical geodesic. We will now recall some properties on this matter, which will be used later in §3. Let $\gamma: I\to\partial\Sigma$ be a vertical geodesic with unit speed such that $\gamma'=\partial_t$ (this orientation of vertical geodesics will be fixed throughout the text), where $I\subset\mathbb{R}$ is an interval, and denote by $\widetilde{\gamma}: I\to\partial\widetilde{\Sigma}$ the conjugate curve, which will be assumed to lie in $\mathbb{H}^2\times\{0\}$ after a vertical translation.

Let us consider the half-space model $\mathbb{H}^2\times\mathbb{R}=\{(x,y,t)\in\mathbb{R}^3: y>0\}$, whose metric is given by $y^{-2}\left(\mathrm{d}x^2+\mathrm{d}y^2\right)+\mathrm{d}t^2$, with positively oriented orthonormal frame $\{E_1,E_2,\partial_t\}$ given by $E_1=y\partial_x$ and $E_2=y\partial_y$ (observe that E_1 is tangent to the foliation of $\mathbb{H}^2$ by horocycles $y=y_0$, with $y_0>0$). Since γ is vertical and $\widetilde{\gamma}$ lies in a horizontal slice, there exist smooth functions $\psi,\theta\in C^\infty(I)$ such that

$$N_{\gamma(t)}=\cos(\psi(t))E_1+\sin(\psi(t))E_2, \tag{2.1}$$

$$\widetilde{\gamma}'(t)=\cos(\theta(t))E_1+\sin(\theta(t))E_2, \tag{2.2}$$

called, respectively, the angle of rotation of N along γ and the angle of rotation of $\widetilde{\gamma}$ with respect to the foliation by horocycles. We now collect some relations between these quantities (see also [1, 9, 19]).

Observe that E_1 and E_2 are parallel vector fields along γ, since they satisfy $\overline{\nabla}_{\partial_t}E_1=\overline{\nabla}_{\partial_t}E_2=0$, where $\overline{\nabla}$ stands for the ambient Levi-Civita connection. This is due to the facts that that $\mathbb{H}^2\times\mathbb{R}$ is a Riemannian product and E_1 and E_2 do not depend on the variable t. By taking derivatives in equation (2.1), we get $\overline{\nabla}_{\gamma'}N=-\psi'\sin(\psi)E_1+\psi'\cos(\psi)E_2=-\psi'N\times\gamma'$, where $\times$ is the cross-product in $\mathbb{H}^2\times\mathbb{R}$. Using the properties of the conjugation, we deduce the identity

$$\psi'=-\left\langle\overline{\nabla}_{\gamma'}N,N\times\gamma'\right\rangle=\langle S\gamma',J\gamma'\rangle=-\left\langle J\widetilde{S}\widetilde{\gamma}',J\widetilde{\gamma}'\right\rangle=\left\langle\overline{\nabla}_{\widetilde{\gamma}'}\widetilde{N},\widetilde{\gamma}'\right\rangle=-\kappa_g, \tag{2.3}$$

where κ_g is the geodesic curvature of $\widetilde{\gamma}$ as a curve of $\mathbb{H}^2\times\{0\}$ with respect to the conormal $\widetilde{N}$ (recall that $\widetilde{\Sigma}$ intersects $\mathbb{H}^2\times\{0\}$ orthogonally). Now we will obtain further information under the additional assumption that the surfaces are *multigraphs* – that is, their common angle function ν has a sign.

Lemma 1. *Assume that the interiors of* Σ *and* $\widetilde{\Sigma}$ *are multigraphs over (possibly nonembedded) domains* Ω *and* $\widetilde{\Omega}$*, respectively, with angle function* $\nu>0$*, and let* γ *be a vertical geodesic in* $\partial\Sigma$ *with* $\gamma'=\partial_t$*. In the notation already given:*

(a) *If* $\psi'>0$*, then* $J\gamma'$ *(resp.,* $J\widetilde{\gamma}'=\partial_t$*) is a unit outer conormal to* Σ*(resp.,* $\widetilde{\Sigma}$*) along* γ *(resp.* $\widetilde{\gamma}$*),* $\widetilde{N}$ *points to the interior of* $\widetilde{\Omega}$ *along* $\widetilde{\gamma}$*, and* $\widetilde{\Sigma}$ *lies in* $\mathbb{H}^2\times(-\infty,0]$ *locally around* $\widetilde{\gamma}$ *(see Figure 1, top).*

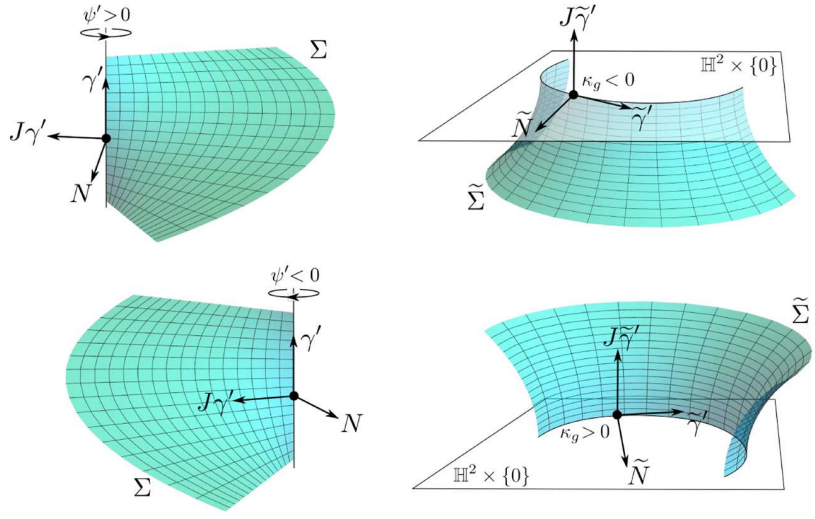

Figure 1. Orientation of the conjugate surfaces Σ and $\widetilde{\Sigma}$ according to the direction of rotation of N along a vertical geodesic γ.

(b) *If $\psi' < 0$, then $J\gamma'$ (resp., $J\widetilde{\gamma}' = \partial_t$) is a unit inner conormal to Σ(resp. $\widetilde{\Sigma}$) along γ (resp. $\widetilde{\gamma}$), $\widetilde{N}$ points to the exterior of $\widetilde{\Omega}$ along $\widetilde{\gamma}$, and $\widetilde{\Sigma}$ lies in $\mathbb{H}^2 \times [0, +\infty)$ locally around $\widetilde{\gamma}$ (see Figure 1, bottom).*

Either way, the identity $\theta' = \psi' - \cos(\theta)$ holds true.

Proof. We will prove only (a), since (b) is analogous, so we will suppose that $\psi' > 0$. Observe that the normal N points upward in the interior of Σ, which is locally a graph by the assumption $\nu > 0$. This argument is not valid along γ, where $\nu = 0$, but we infer by continuity that N is a horizontal $\frac{\pi}{2}$-rotation of the outer unit conormal to Σ along γ (this rotation is counterclockwise in a horizontal slice, in view of the condition $\psi' > 0$). Hence, $J\gamma' = N \times \gamma'$ is determined by the ambient orientation and points outside Σ along γ, as depicted in Figure 1 (top left). Since the rotation J is intrinsic, we deduce that $J\widetilde{\gamma}'$ points outside $\widetilde{\Sigma}$ along $\widetilde{\gamma}$, and $\widetilde{N} = \widetilde{\gamma}' \times J\widetilde{\gamma}'$ is also determined, as shown in Figure 1 (top right).

Assume now by contradiction that $\widetilde{N}$ points to the exterior of $\widetilde{\Omega}$ at some point p of $\widetilde{\gamma}$. Since $\kappa_g = -\psi' < 0$ with respect to the conormal $\widetilde{N}$ and $\nu > 0$, we infer that $\widetilde{\Sigma}$ projects locally into the convex side of $\widetilde{\gamma}$. This yields a contradiction with the boundary maximum principle by comparing $\widetilde{\Sigma}$ and a vertical plane tangent to $\widetilde{\gamma}$ at p. Note that $J\widetilde{\gamma}'$ cannot be equal to $-\partial_t$ (so it must be $J\widetilde{\gamma}' = \partial_t$) because it points outside $\widetilde{\Sigma}$ along $\widetilde{\gamma}$ and the angle function is positive. As a consequence, a neighborhood of $\widetilde{\gamma}$ in $\widetilde{\Sigma}$ is contained in $\mathbb{H}^2 \times (-\infty, 0]$.

It is easy to calculate $\overline{\nabla}_{E_1} E_1 = E_2$, $\overline{\nabla}_{E_1} E_2 = -E_1$, and $\overline{\nabla}_{E_2} E_1 = \overline{\nabla}_{E_2} E_2 = 0$ by using the expressions of E_1 and E_2 and the Koszul formula. On the one hand, this allows us to take derivatives in equation (2.2) to obtain $\overline{\nabla}_{\widetilde{\gamma}'} \widetilde{\gamma}' = (\theta' + \cos(\theta))(-\sin(\theta) E_1 + \cos(\theta) E_2)$.

On the other hand, the foregoing discussion shows that $\widetilde{N}=\widetilde{\gamma}'\times J\widetilde{\gamma}'=\widetilde{\gamma}'\times\partial_t=\sin(\theta)E_1-\cos(\theta)E_2$, so the last identity in the statement follows from plugging these computations in the expression $-\psi'=\kappa_g=\langle\overline{\nabla}_{\widetilde{\gamma}'}\widetilde{\gamma}',\widetilde{N}\rangle$. □

3. Construction of genus 1 saddle towers and *k*-noids

The first part of this section is devoted to proving Theorems 1 and 2. The arguments leading to these results are based on a conjugate construction that depends on a parameter $0<l\leq\infty$ that will be fixed henceforth. The case $0<l<\infty$ gives the saddle towers whose fundamental pieces lie in a slab of height l, whereas the case $l=\infty$ gives rise to the k-noids. Although a limit argument for $l\to\infty$ would imply the latter (as in [16]), we will discuss both cases together.

3.1. The conjugate construction

Let Δ be a geodesic triangle with sides ℓ_1, ℓ_2, and ℓ_3 and opposite vertices p_1, p_2, and p_3. Assume that Δ is acute and the length of ℓ_2 is given by the aforesaid parameter $l\in(0,\infty]$, so that p_1 is ideal if $l=\infty$. Therefore Δ is determined by the length a of ℓ_1 and by the angle φ at p_2. Given $b\in\mathbb{R}$, consider the unique solution $\Sigma(a,\varphi,b)$ to the Jenkins–Serrin problem over Δ with boundary values b along ℓ_1, $+\infty$ along ℓ_2, and 0 along ℓ_3. The existence and uniqueness of such a solution are guaranteed under these boundary conditions (see [14] and the references therein). In particular, the interior of $\Sigma(a,\varphi,b)$ is a minimal graph over Δ whose boundary consists of two horizontal geodesics h_1 and h_3 lying in $\mathbb{H}^2\times\{b\}$ and $\mathbb{H}^2\times\{0\}$, respectively, and three vertical geodesics v_1, v_2, and v_3 projecting onto p_1, p_2, and p_3, respectively. Note that v_1 is an ideal vertical half-geodesic, provided that $l=\infty$. The boundary of $\Sigma(a,\varphi,b)$ also contains an horizontal ideal half-geodesic $h_2\subset\mathbb{H}^2\times\{+\infty\}$ projecting onto ℓ_2.

Since $\Delta\subset\mathbb{H}^2$ is convex, the conjugate minimal surface $\widetilde{\Sigma}(a,\varphi,b)\subset\mathbb{H}^2\times\mathbb{R}$ is a graph over some domain $\widetilde{\Delta}\subset\mathbb{H}^2$ due to the Krust-type theorem in [8]. The normal N along v_2 or v_3 rotates counterclockwise, so theoretical conjugate curves $\widetilde{v}_2$ and $\widetilde{v}_3$ lie in horizontal planes and are convex toward the exterior of $\widetilde{\Delta}$ by Lemma 1. This lemma also implies that $\widetilde{\Sigma}(a,\varphi,b)$ lies locally below the horizontal slices containing $\widetilde{v}_2$ and $\widetilde{v}_3$. We will assume that $\widetilde{v}_3\subset\mathbb{H}^2\times\{0\}$ in the sequel. As for horizontal geodesics, the conjugate curve $\widetilde{h}_i$ of h_i, $i\in\{1,2,3\}$, can be decomposed component-wise as $\widetilde{h}_i=(\beta_i,z_i)\in\mathbb{H}^2\times\mathbb{R}$ and lies in a vertical plane P_i. Since Σ is orthogonal to P_i along $\widetilde{h}_i$, it follows that $\{\gamma_i',N\}$ is an orthonormal frame along $\widetilde{h}_i$ as a curve of P_i. Hence,

$$|z_i'|=|\langle\gamma_i',\partial_t\rangle|=\sqrt{1-\langle N,\partial_t\rangle^2}=\sqrt{1-\nu^2},$$

from which we also deduce that $\|\beta_i'\|=\sqrt{1-z_i^2}=|\nu|$. Therefore, points at which ν takes the values 0 or ±1 will be the key to understanding the behavior of $\widetilde{h}_i$, for they are the points where the components β_i and z_i may fail to be one-to-one.

Lemma 2. *The angle function ν of $\Sigma(a,\varphi,b)$ is zero precisely at $v_2\cup v_3$ if $l=\infty$ or $v_1\cup v_2\cup v_3$ if $l<\infty$. Furthermore, there is exactly one point of $\Sigma(a,\varphi,b)$ with $\nu=1$, and it belongs to h_1.*

Proof. We will write $\Sigma = \Sigma(a,\varphi,b)$ throughout this proof for simplicity. The interior of Σ is a graph, so there are no interior zeros of ν. Besides, zeros in the interior of some h_i would contradict the boundary maximum principle by comparing Σ and the vertical plane $\ell_i \times \mathbb{R}$.

Let us suppose now that $\nu(p) = 1$ at some interior point p, and assume first that $l < \infty$. The intersection of Σ and the horizontal slice S containing p is an equiangular set of curves with at least four curves starting at p. These curves do not enclose relatively compact regions in the interior Σ (which is a graph), by a standard application of the maximum principle with respect to horizontal slices. By looking at the boundary of Σ, one easily infers that two of the curves starting at p must reach some h_i or have a common endpoint at some v_i. Note that Σ extends analytically by axial symmetry about its boundary components, so this set of curves is part of the (also equiangular) intersection of S and the extended Σ. In particular, no two of the curves starting at p can reach the same v_i, for they would intersect it at the same point, in contradiction with the fact that S is not tangent to Σ at any point of v_i. Since $S \cap \Sigma$ cannot reach the interiors of v_2 and v_3 simultaneously (for they lie at different heights), it follows that two of the curves starting at p must reach some h_i. Therefore, the segment of h_i joining the corresponding two end points is also in the intersection $S \cap \Sigma$, producing a similar contradiction with the maximum principle.

The case $l = \infty$ is similar, provided that we discard the possibility that two of the curves in $S \cap \Sigma$ starting at p asymptotically reach v_1. Were that the case, the region $\Omega \subset \mathbb{H}^2$ enclosed by the projection of these two curves would have an end of type 1 in the sense of [14, Definition 4.14] (these projected curves are asymptotic to each other at the ideal projection of v_1 because they lie inside Δ). The general maximum principle [14, Theorem 4.16] applies in comparing the graphical surfaces Σ and S over Ω, which have the same (constant) boundary values.

Let us finally deal with boundary points at which $\nu = 1$. They cannot occur at h_3, because of the boundary maximum principle (compare Σ and the slice $\mathbb{H}^2 \times \{0\}$). As for h_1, recall that Σ can be extended analytically by axial symmetry about its boundary to a complete surface, so the normal N (with the assumption $\nu > 0$) points toward Δ at the end point $h_1 \cap v_2$ and toward the opposite direction at $h_1 \cap v_3$ (recall that the interior of Σ is a graph over the triangle Δ, so its interior angles at the corners $h_1 \cap v_2$ and $h_1 \cap v_3$ equal $\frac{\pi}{2}$, since Σ cannot approach h_1 from outside Δ). This means that N rotates an angle of π along h_1 as sketched in Figure 2, giving rise to at least one point of h_1 where $\nu = 1$ (when N has rotated just $\frac{\pi}{2}$). If there were more than one such point, then the intersection of Σ and the horizontal slice containing h_1 would also contain two interior curves starting at these two points, and we would get a region bounded by horizontal curves and a similar contradiction with the maximum principle as in the previous arguments. □

We deduce that $\widetilde{h}_3$ projects one-to-one into the factors $\mathbb{H}^2$ and $\mathbb{R}$, as well as $\widetilde{h}_1$ into the factor $\mathbb{H}^2$. However, the component of $\widetilde{h}_1$ in the factor $\mathbb{R}$ has a minimum at the unique point where $\nu = 1$. We remark that the end points of $\widetilde{h}_1$ cannot be critical for the height, since Σ reaches the slices containing $\widetilde{v}_2$ and $\widetilde{v}_3$ orthogonally from below by Lemma 1 (see Figure 2). On the other hand, the conjugate curve $\widetilde{h}_2$ can be thought of as an ideal vertical

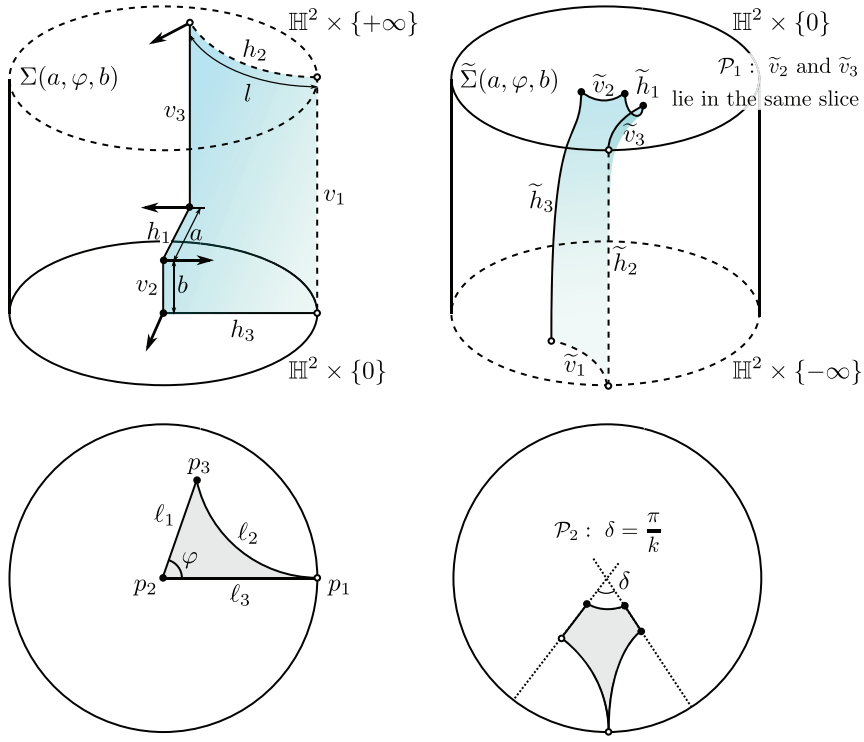

Figure 2. Conjugate surfaces $\Sigma(a,\varphi,b)$ and $\widetilde{\Sigma}(a,\varphi,b)$ and their domains Δ and $\widetilde{\Delta}$ in $\mathbb{H}^2$ in the case $l = \infty$. Dashed lines represent ideal geodesics, and white dots represent ideal vertices. The arrows in $\Sigma(a,\varphi,b)$ represent the normal N at the end points of v_2 and v_3, which rotates counterclockwise along both geodesics.

segment of length l in $\partial_\infty \mathbb{H}^2 \times \mathbb{R}$. Since $\Sigma(a,\varphi,b)$ becomes vertical when one approaches the side ℓ_2, the length of the ideal vertical half-geodesic $\widetilde{h}_2$ is equal to l; in particular, $\widetilde{v}_1 \subset \mathbb{H}^2 \times \{-l\}$. If $l < \infty$, then N rotates clockwise along v_1, so the conjugate curve $\widetilde{v}_1$ lies in a horizontal slice (which $\Sigma(a,\varphi,b)$ approaches from above) and is convex toward the exterior of $\widetilde{\Delta}$, by Lemma 1. If $l = \infty$, then $\widetilde{v}_1$ is an ideal horizontal half-geodesic in $\mathbb{H}^2 \times \{-\infty\}$ (see also [1, Corollary 2.4]). A depiction of the conjugate surfaces is given in Figure 2.

We would like $\widetilde{v}_2$ and $\widetilde{v}_3$ to be contained in the same horizontal plane, as well as for the complete geodesics of $\mathbb{H}^2$ containing $\widetilde{h}_1$ and $\widetilde{h}_3$ to intersect at an angle of $\frac{\pi}{k}$ (as shown in Figure 2, bottom right). Such a configuration would lead to the desired construction of saddle towers and k-noids after reflection of the fundamental piece $\widetilde{\Sigma}$ across its boundary, so we need to find values of (a,φ,b) that solve the following period problems, inspired by the arguments in [19]:

(1) **First period problem.** Let $\mathcal{P}_1(a,\varphi,b)$ be the difference of heights of the horizontal curves $\widetilde{v}_2$ and $\widetilde{v}_3$ – that is, the difference of heights of the end points of $\widetilde{h}_1$.

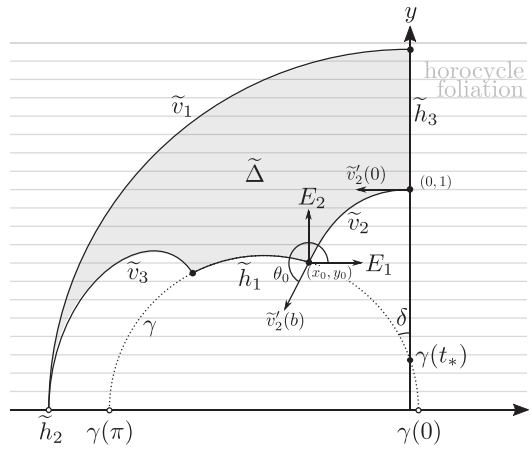

Figure 3. The angle θ_0 of rotation of $\widetilde{v}_2$ with respect to the horocycle foliation at $\widetilde{v}_2(b)$, where we identify $\mathbb{H}^2\times\{0\}$ and $\mathbb{H}^2$. The surface $\widetilde{\Sigma}(a,\varphi,b)$ projects onto the shaded region $\widetilde{\Delta}$, with boundary the projections of the labeled curves. The complete geodesic γ containing the projection of $\widetilde{h}_1$ appears as the dotted line.

Parametrizing $\widetilde{h}_1:[0,a]\to\mathbb{H}^2\times\mathbb{R}$ with $\widetilde{h}_1(0)\in\widetilde{v}_2$, $\widetilde{h}_1(a)\in\widetilde{v}_3$, and unit speed, by means of the properties of the conjugation, we can express

$$\mathcal{P}_1(a,\varphi,b)=\int_{\widetilde{h}_1}\left\langle \widetilde{h}_1',\partial_t\right\rangle=\int_{h_1}\langle\eta,\partial_t\rangle, \tag{3.1}$$

where $\eta=-Jh_1'$ is the unit inward conormal vector to $\Sigma(a,\varphi,b)$ along h_1.

(2) **Second period problem.** Let us work in the half-space model. After an ambient isometry, we can assume that $\widetilde{h}_3$ lies in the vertical plane $x=0$ and $\widetilde{v}_2:[0,b]\to\mathbb{H}^2\times\mathbb{R}$ is contained in the horizontal plane $t=0$ with end points $\widetilde{v}_2(0)\in\widetilde{h}_3$ and $\widetilde{v}_2(b)\in\widetilde{h}_1$. Expressing in coordinates $\widetilde{v}_2(t)=(x(t),y(t),0)$, we can also assume that $(x(0),y(0))=(0,1)$ and $x(t)<0$ when t is close to 0 (since $\widetilde{v}_2$ and $\widetilde{h}_3$ are orthogonal; see Figure 3). We will write $(x(b),y(b))=(x_0,y_0)$ for simplicity. Recall that this parametrization comes (via conjugation) from the chosen orientation, in which $v_2'=\partial_t$.

Let $\theta\in\mathcal{C}^\infty[0,b]$ be the angle of rotation of $\widetilde{v}_2$ with respect to the horocycle foliation in the sense of equation (2.2), where we choose the initial angle $\theta(0)=\pi$. We will call $\theta_0=\theta(b)$ and assume in what follows that $\pi<\theta(t)<2\pi$ and $x(t)<0$ if $0<t\le b$ (these inequalities will hold true by Lemma 6). The complete geodesic $\gamma\subset\mathbb{H}^2$ containing the projection of $\widetilde{h}_1$ can be parametrized as

$$\gamma:(0,\pi)\to\mathbb{H}^2,\quad \gamma(t)=\left(x_0-y_0\frac{\cos(t)+\cos(\theta_0)}{\sin(\theta_0)},-y_0\frac{\sin(t)}{\sin(\theta_0)}\right). \tag{3.2}$$

Note that $\gamma(\theta_0-\pi)=(x_0,y_0)$ and $\gamma'(\theta_0-\pi)=\frac{-1}{\sin(\theta_0)}(\sin(\theta_0)E_1-\cos(\theta_0)E_2)$. If γ meets the y-axis at the point $\gamma(t_*)$, we define the second period as the cosine of the (nonoriented) angle δ at $\gamma(t_*)$ subtended by the arc $\widetilde{v}_2$ (see Figure 3). From the

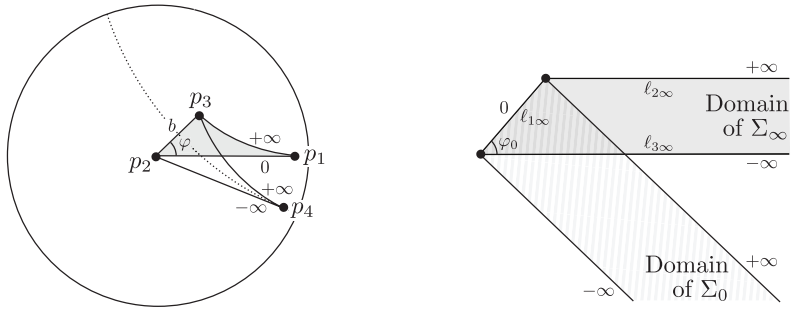

Figure 4. On the left, boundary values for Jenkins–Serrin problems in $\mathbb{H}^2$ solved by $\Sigma(a,\varphi,b)$ and $\Sigma_0(b)$, where the perpendicular bisector of ℓ_1 is represented as a dotted line and $l < \infty$. On the right, the limit $\Sigma_\infty \subset \mathbb{R}^3$ by rescaling (fixing the length of ℓ_1 equal to 1) and the helicoid $\Sigma_0 \subset \mathbb{R}^3$ in the proof of Lemma 5.

parametrization (3.2), we can compute

$$\mathcal{P}_2(a,\varphi,b) = \cos(\delta) = \frac{\langle \gamma'(t_*), E_2 \rangle}{|\gamma'(t_*)|} = \cos(t_*) = \frac{x_0 \sin(\theta_0)}{y_0} - \cos(\theta_0). \tag{3.3}$$

However, the right-hand side of equation (3.3) makes sense (and we will take it as the definition of $\mathcal{P}_2$) even though there is no such intersection point. Lemma 6 will show that if $\mathcal{P}_1(a,\varphi,b) = 0$ and $\mathcal{P}_2(a,\varphi,b) = \cos\left(\frac{\pi}{k}\right)$ for some $k \geq 3$, then γ and the positive y-axis do intersect, with angle $\delta = \frac{\pi}{k}$.

The uniqueness of the solution of the Jenkins–Serrin problem implies that $\widetilde{\Sigma}(a,\varphi,b)$ depends smoothly on the parameters (a,φ,b), in the sense that given a sequence (a_n,φ_n,b_n) converging to some (a,φ,b), the sequence of surfaces with boundary $\widetilde{\Sigma}(a_n,\varphi_n,b_n)$ converges in the $\mathcal{C}^k$-topology to $\widetilde{\Sigma}(a,\varphi,b)$ for all $k \geq 0$. This follows from standard convergence arguments for minimal graphs along with the continuity of the conjugation (see [16, Proposition 2.10] or [1, Proposition 2.3]).

3.2. Solving the period problems

In the sequel we will assume that b is any nonnegative real number and that (a,φ) lies in the domain

$$\Omega = \left\{(a,\varphi) \in \mathbb{R}^2 : 0 < \varphi < \tfrac{\pi}{2}, 0 < a < a_{\max}(\varphi)\right\},$$

where

$$a_{\max}(\varphi) = 2\,\mathrm{arc\ tanh}\left(\tanh(l)\cos(\varphi)\right), \tag{3.4}$$

and $\tanh(l) = 1$ whenever $l = \infty$. The condition $0 < a < a_{\max}(\varphi)$ means that the angle of Δ at p_3 is always greater than φ, and then an isosceles triangle Δ_0 with vertices p_2, p_3, p_4, and $d(p_2,p_4) = d(p_3,p_4) = l$ intersects Δ as in Figure 4 (the vertex p_4 is ideal, provided that $l = \infty$). Note that $a_{\max}(\varphi)$ is the length of the unequal side of an isosceles triangle whose equal sides have length l and whose equal angles are equal to φ, so formula (3.4)

easily follows from the fact that the cosine of an angle of a hyperbolic right triangle is the quotient of the hyperbolic tangents of the adjacent side and the hypotenuse.

Remark 1. The restriction $(a,\varphi) \in \Omega$ is used in Lemma 5 to compare $\Sigma(a,\varphi,b)$ with a solution of a Jenkins–Serrin problem over Δ_0 and to solve the first period problem. Similar arguments to those in Lemma 5 show that if $a > a_{\max}(\varphi)$, then the first period problem has no solution, so the condition $(a,\varphi) \in \Omega$ is natural.

Lemma 3. *$\mathcal{P}_1 : \Omega \times \mathbb{R}^+ \to \mathbb{R}$ is a continuous and strictly decreasing function with respect to the third argument b.*

Proof. Consider two surfaces $\Sigma_1 = \Sigma(a,\varphi,b_1)$ and $\Sigma_2 = \Sigma(a,\varphi,b_2)$ with $0 < b_1 < b_2$. Let us translate each Σ_i vertically so that it takes the values 0 along ℓ_1 and $-b_i$ along ℓ_3. The surface Σ_1 lies above Σ_2, and we can compare the vertical components of their inward-pointing conormals η_1 and η_2, which satisfy $\langle \eta_2, \partial_t \rangle < \langle \eta_1, \partial_t \rangle$ in the interior of h_1 by the boundary maximum principle. In particular,

$$\mathcal{P}_1(a,\varphi,b_2) = \int_{h_1} \langle \eta_2, \partial_t \rangle < \int_{h_1} \langle \eta_1, \partial_t \rangle = \mathcal{P}_1(a,\varphi,b_1). \qquad \square$$

In the proof of Lemma 5, we need a Jenkins–Serrin solution over Δ_0 to have radial limits as we approach a vertex of Δ_0. To this end, we will state a more general result (we also point out that it extends easily to other $\mathbb{E}(\kappa,\tau)$-spaces):

Lemma 4. *Let $\Omega \subset \mathbb{H}^2$ be an open domain with piecewise regular boundary, and assume that β_1 and β_2 are two regular components of $\partial\Omega$ that meet in a common vertex $p \in \partial\Omega$ with interior angle $0 < \alpha < 2\pi$. Suppose that $u \in \mathcal{C}^\infty(\Omega)$ is a solution to the minimal surface equation over Ω with bounded continuous limit values along β_1 and asymptotic value $+\infty$ or $-\infty$ along β_2. Then u has finite radial limits at p along any geodesic segment interior to Ω and not tangent to β_1 or β_2.*

Proof. Let γ be the vertical geodesic segment projecting onto p and lying in the boundary of Σ, the minimal surface spanned by u. Observe that Σ extends analytically across γ by axial symmetry, so the normal N (with $\nu > 0$ at the interior of Σ) extends smoothly to γ. Moreover, N rotates monotonically along γ because Σ is a graph, as a consequence of the boundary maximum principle for minimal surfaces. Therefore, the conormal $J\gamma' = N \times \gamma'$ also rotates monotonically along γ (see Figure 1). Since $J\gamma'$ is horizontal and tangent to the level curves of the height function of Σ, we deduce that the projections of such level curves form an open book foliation of a neighborhood of p with binding at p.

This implies that when we approach p along an interior geodesic σ not tangent to β_1 or β_2, the limit of u will be precisely the value of u at the unique level curve (in the aforesaid foliation) tangent to σ at p, so the desired limit exists and is finite. $\square$

Lemma 5. *There exists a unique function $f : \Omega \to \mathbb{R}_+$ such that $\mathcal{P}_1(a,\varphi,f(a,\varphi)) = 0$ for all $(a,\varphi) \in \Omega$. Furthermore,*

(a) *f is a continuous function;*

(b) *given* $\varphi_0\in\left(0,\frac{\pi}{2}\right)$,

$$\lim_{a\to a_{\max}(\varphi_0)} f(a,\varphi_0)=+\infty, \qquad \lim_{(a,\varphi)\to(0,\varphi_0)} f(a,\varphi)=0.$$

Proof. Fix $(a,\varphi)\in\Omega$. Let p_4 be the point in the perpendicular bisector of the segment ℓ_1 with $d(p_2,p_4)=d(p_3,p_4)=l$, such that the triangle Δ_0 with vertices p_1, p_2, and p_4 lies on the same side of ℓ_1 as Δ (see Figure 4). Let $\Sigma_0(b)$ be the unique solution to the Jenkins–Serrin problem over the triangle Δ_0 with values b along the segment $\overline{p_2p_3}$, $+\infty$ along $\overline{p_3p_4}$, and $-\infty$ along $\overline{p_2p_4}$. Since $(a,\varphi)\in\Omega$, then $\Delta\cap\Delta_0\subset\mathbb{H}^2$ is a bounded geodesic triangle with vertices p_2, p_3, and $q\in\ell_3$. Lemma 4 says that $\Sigma_0(b)$ has a finite radial limit at p_2 along ℓ_3 as a graph over Δ_0, and likewise $\Sigma(a,\varphi,b)$ has a finite radial limit at p_3 along $\overline{p_3p_4}$ for all b (whereas $\Sigma_0(b)$ has value $+\infty$ along this segment). Therefore, if b is large enough, then $\Sigma_0(b)$ is above $\Sigma(a,\varphi,b)$ over the boundary of $\Delta\cap\Delta_0$. By the maximum principle, it is also above $\Sigma(a,\varphi,b)$ in the interior of $\Delta\cap\Delta_0$. In particular, we get that $\Sigma\cap\Sigma_0(b)=h_1\cup v_2\cup v_3$ when b is large.

This means that we can compare the vertical components of the inward-pointing conormals η and η_0 of $\Sigma(a,\varphi,b)$ and $\Sigma_0(b)$, respectively, along the curve h_1 (as in Lemma 3). By the boundary maximum principle for minimal surfaces, we get the strict inequality $\langle\eta,\partial_t\rangle<\langle\eta_0,\partial_t\rangle$ in the interior of h_1, and hence

$$\mathcal{P}_1(a,\varphi,b)=\int_{h_1}\langle\eta,\partial_t\rangle<\int_{h_1}\langle\eta_0,\partial_t\rangle=0, \tag{3.5}$$

provided that b is large enough. The last integral in this equation vanishes because $\Sigma_0(b)$ is axially symmetric with respect to the perpendicular bisector of h_1 in $\mathbb{H}^2\times\{b\}$.

Due to the continuity of $\Sigma(a,\varphi,b)$ with respect to the parameters (a,φ,b), the surfaces $\Sigma(a,\varphi,b)$ converge to $\Sigma(a,\varphi,0)$ as $b\to 0$. We have $\mathcal{P}_1(a,\varphi,0)>0$, since $\Sigma(a,\varphi,0)$ lies above the horizontal surface $\Delta\times\{0\}$ by the maximum principle, and we can compare the third coordinate of their conormals along the common boundary h_1 by the boundary maximum principle (note that the third coordinate of the conormal of $\Delta\times\{0\}$ identically vanishes). By the continuity and monotonicity of $\mathcal{P}_1$ with respect to b proved in Lemma 3, there exists a unique $b_0\in\mathbb{R}^+$ such that $\mathcal{P}_1(a,\varphi,b_0)=0$. Hence this defines unequivocally $f(a,\varphi)=b_0$. The continuity of f is a consequence of its uniqueness. If (a_n,φ_n) and (a_n',φ_n') are two sequences in Ω converging to some $(a_\infty,\varphi_\infty)\in\Omega$ such that, after passing to a subsequence, $f(a_n,\varphi_n)\to b_\infty$ and $f(a_n',\varphi_n')\to b_\infty'$, then $\mathcal{P}_1(a_\infty,\varphi_\infty,b_\infty)=\mathcal{P}_1(a_\infty,\varphi_\infty,b_\infty')=0$ implies $b_\infty=b_\infty'$, and item (a) is proved.

As for the first limit in (b), assume by contradiction that there is a sequence $a_n\to a_{\max}(\varphi_0)$ such that $f(a_n,\varphi_0)$ converges, after passing to a subsequence, to some $b_\infty\in[0,+\infty)$. The surface $\Sigma_0(b_\infty)$ lies below $\Sigma(a_{\max}(\varphi_0),\varphi,b_\infty)$ as graphs over their common domain $\Delta=\Delta_0$ by the maximum principle, because their boundary values are ordered likewise. Note that they have a common value b_∞ along ℓ_1, so their inward-pointing conormals can be compared along h_1 again by the boundary maximum principle. Since the $\Sigma_0(b_\infty)$ has zero period because of its symmetry, this contradicts the fact that $\Sigma(a_{\max}(\varphi_0),\varphi,b_\infty)$ also has zero period.

We will compute the limit as (a,φ) approaches $(0,\varphi_0)$ again by contradiction, so let us assume that there is a sequence (a_n,φ_n) tending to $(0,\varphi_0)$ such that (after passing to a subsequence) $f(a_n,\varphi_n)\to b_\infty$, with $b_\infty\in(0,+\infty]$. Let us translate the surfaces $\Sigma(a_n,\varphi_n,f(a_n,\varphi_n))$ vertically so that they take zero value along ℓ_1 and $-f(a_n,\varphi_n)$ along ℓ_3. Since $a_n\to 0$, we can blow up the surface and the metric of $\mathbb{H}^2\times\mathbb{R}$ in such a way that a_n is equal to 1. The new sequence of rescaled surfaces converges in the $\mathcal{C}^k$-topology for all k to a minimal surface Σ_∞ in Euclidean space $\mathbb{R}^3$. This surface Σ_∞ is a graph over a domain of $\mathbb{R}^2$ bounded by three lines $\ell_{1\infty}$, $\ell_{2\infty}$, and $\ell_{3\infty}$ such that $\ell_{2\infty}$ and $\ell_{3\infty}$ are parallel and $\ell_{1\infty}$ makes an angle of φ_0 with $\ell_{2\infty}$. Moreover, Σ_∞ takes values $+\infty$ along $\ell_{2\infty}$, $-\infty$ along $\ell_{3\infty}$ (since $b_\infty>0$), and 0 along $\ell_{1\infty}$. Let us consider Σ_0 the helicoid of $\mathbb{R}^3$ with axis $\ell_{1\infty}$ which is a graph over a half-strip of $\mathbb{R}^2$, as depicted in Figure 4 (right). Since $0<\varphi_0<\frac{\pi}{2}$, the intersection of the domains of Σ_0 and Σ_∞ is a triangle on whose sides the boundary values of Σ_0 are greater than or equal to the corresponding values of Σ_∞. By the maximum principle, we deduce that Σ_0 lies above the surface Σ_∞ also in the interior of that triangle. Hence, we can compare their conormals along $\ell_{1\infty}$ by the boundary maximum principle to conclude that the period of Σ_∞ is not zero, which contradicts the assertion that each of the surfaces $\Sigma(a_n,\varphi_n,f(a_n,\varphi_n))$ has zero period. □

This solves the first period problem, and we will now focus on the second one. To this end, we will use the notation defined in Section 3.1 (see also Figure 3).

Lemma 6. *Set $\varphi_0\in\left(0,\frac{\pi}{2}\right)$ and $a\in(0,a_{\max}(\varphi_0))$.*

(a) *The inequalities $x(t)<0$ and $\pi<\theta(t)<2\pi$ hold true for all $t\in(0,b]$.*

(b) *If the curve γ intersects the positive y-axis with angle δ, then $\delta<\varphi_0$, in which case $\mathcal{P}_2(a,\varphi_0,f(a,\varphi_0))=\cos(\delta)$.*

(c) *If $\mathcal{P}_2(a,\varphi_0,f(a,\varphi_0))=\cos(\delta)$ for some $\delta\in(0,\varphi_0)$, then γ intersects the positive y-axis with angle δ.*

(d) *If $\mathcal{P}_2(a,\varphi_0,f(a,\varphi_0))=1$, then γ and the y-axis are asymptotic geodesics intersecting at the ideal point $(0,0)$.*

Furthermore,

$$\lim_{a\to 0}\mathcal{P}_2(a,\varphi_0,f(a,\varphi_0))=\cos(\varphi_0),\qquad \lim_{a\to a_{\max}(\varphi_0)}\mathcal{P}_2(a,\varphi_0,f(a,\varphi_0))=+\infty.$$

Proof. We will identify $\widetilde{v}_2$ with its projection to $\mathbb{H}^2$ for the sake of simplicity. Therefore, $\widetilde{v}_2$ is strictly convex (in the hyperbolic geometry) toward the exterior of $\widetilde{\Delta}$ by Lemma 1, and this implies that any geodesic tangent to $\widetilde{v}_2$ lies locally in the interior of $\widetilde{\Delta}$ except for the point of tangency. In particular, we have that $\theta(t)>\pi$ for t close to 0 by just comparing $\widetilde{v}_2$ with the tangent geodesic at $\widetilde{v}_2(0)=(0,1)$ (see Figure 5, left). Furthermore, if $\theta(t)>\pi$ does not hold for all $t\in(0,b]$, then at the smallest $t_0>0$ such that $\theta(t_0)=\pi$, the tangent geodesic has points outside $\widetilde{\Delta}$ arbitrarily close to $\widetilde{v}_2(t_0)$, which is a contradiction (see Figure 5, left).

Assume by contradiction that $x(t)<0$ does not hold in general, and let $t_0\in(0,b]$ be the smallest value such that $x(t_0)=0$, so the curve $\widetilde{v}_2$ between 0 and t_0 together with a segment of the y-axis enclose a bounded domain $U\subset\mathbb{H}^2$ (see Figure 5, center). The

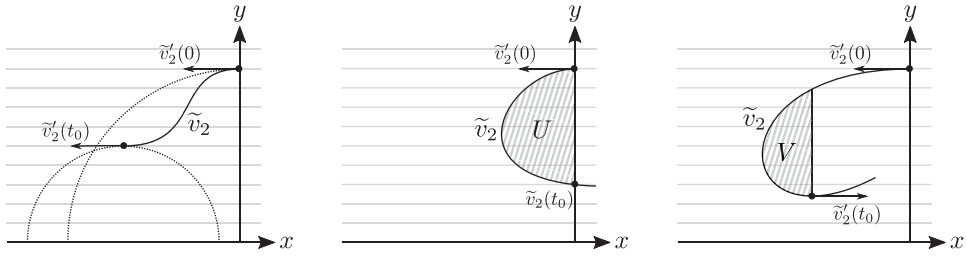

Figure 5. Tangent geodesics at $\widetilde{v}_2(0)$ and at a first $t_0 \in (0,b]$ such that $\theta(t_0) = \pi$ (left). A first $t_0 \in (0,b]$ such that $x(t_0) = 0$ (center). A first $t_0 \in (0,b]$ such that $\theta(t_0) = 2\pi$ (right). The domains U and V are those where we apply Gauss–Bonnet formula in Lemma 6.

curve $\widetilde{v}_2$ is convex toward the interior of U, and U has two interior angles equal to $\frac{\pi}{2}$ and $\alpha = \theta(t_0) - \frac{3\pi}{2} \in (0,\pi)$, so the Gauss–Bonnet formula yields

$$\begin{aligned} 0 > -\operatorname{area}(U) &= 2\pi + \int_0^{t_0} \kappa_g(t)\mathrm{d}t - \left(\tfrac{\pi}{2} + \pi - \alpha\right) \\ &> \tfrac{\pi}{2} + \int_0^b \kappa_g(t)\mathrm{d}t = \tfrac{\pi}{2} - \int_0^b \psi'(t)\,\mathrm{d}t = \tfrac{\pi}{2} - \varphi_0, \end{aligned} \tag{3.6}$$

where $\kappa_g < 0$ is the geodesic curvature with respect to the unit conormal $\widetilde{N}$ pointing outside $\widetilde{\Delta}$ (see Lemma 1). We have also used the fact that the angle ψ of the normal N along v_2, in the sense of equation (2.1), rotates counterclockwise with $\psi' = -\kappa_g > 0$ and $\psi(b) - \psi(0) = \varphi_0$. Inequality (3.6) contradicts the assumption that $\varphi_0 \in \left(0, \frac{\pi}{2}\right)$.

Let us assume, again by contradiction, that there is (a first) $t_0 \in (0,b]$ such that $\theta(t_0) = 2\pi$. This implies that the normal geodesic to $\widetilde{v}_2$ at t_0 is a straight line parallel to the y-axis. Let $V \subset \mathbb{H}^2$ be the domain enclosed by this line together with an arc of $\widetilde{v}_2$ (see Figure 5, right). Note that V has two interior angles $\alpha \in (0,\pi)$ and $\frac{\pi}{2}$, plus $\widetilde{v}_2$ is convex toward V. Reasoning as in formula (3.6), we get the same contradiction $0 > -\operatorname{area}(V) > \frac{\pi}{2} - \varphi_0$, which finishes the proof of (a).

As for (b), if γ intersects the y-axis with angle δ, then there is a region $W \subset \mathbb{H}^2$ bounded by γ, $\widetilde{v}_2$, and the y-axis. The Gauss–Bonnet formula, in the same fashion as in formula (3.6), gives the inequality $0 > -\operatorname{area}(W) > \delta - \varphi_0$, which is equivalent to $\delta < \varphi_0$. The equality $\mathcal{P}_2(a,\varphi,f(a,\varphi)) = \cos(\delta)$ was given in equation (3.3).

We will now discuss (c) and (d). Note that $\gamma(\pi)$ has negative first coordinate by the foregoing analysis, so γ intersects the y-axis if and only the first coordinate of

$$\gamma(0) = \left(x_0 - y_0 \frac{1+\cos(\theta_0)}{\sin(\theta_0)}, 0\right) \tag{3.7}$$

is positive (here, $\sin(\theta_0) < 0$ because $\pi < \theta_0 < 2\pi$). If there exists $\delta \in (0,\varphi_0)$ such that $\mathcal{P}_2(a,\varphi_0,f(a,\varphi_0)) = \frac{x_0 \sin(\theta_0)}{y_0} - \cos(\theta_0) = \cos(\delta) \in (0,1)$, then the first coordinate in equation (3.7) is positive, and it follows from (b) that the angle at the intersection is precisely δ. If $\mathcal{P}_2(a,\varphi_0,f(a,\varphi_0)) = 1$, then the first coordinate of equation (3.7) vanishes, so γ and the y-axis are asymptotic at the ideal point $(0,0)$.

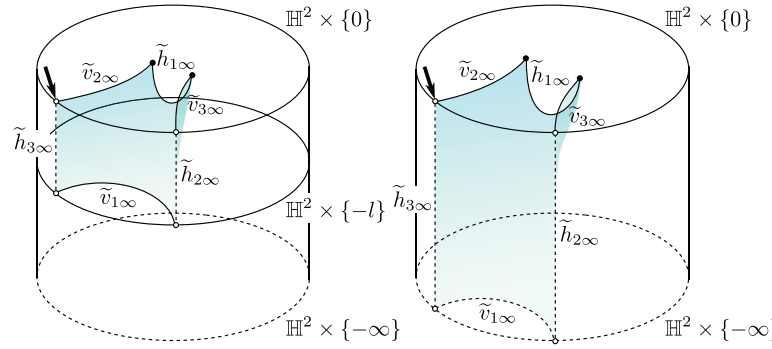

Figure 6. The limit saddle tower ($l < \infty$) and catenoid ($l = \infty$) when $a \to a_{\max}(\varphi_0)$. In the proof of Lemma 6, we bring the points at which the arrows aim to a fixed point of $\mathbb{H}^2$, so we get vertical planes in the limit (instead of the saddle tower or the catenoid).

To finish the proof, let us analyze the limits. Integrating from 0 to b the identity $\theta' = \psi' - \cos(\theta)$ in Lemma 1 (applied to v_2), and taking into account that $\theta(b) - \theta(0) = \theta_0 - \pi$ and $\psi(b) - \psi(0) = \varphi_0$, we get the relation

$$\theta_0 = \varphi_0 + \pi - \int_0^b \cos(\theta(s))\mathrm{d}s. \tag{3.8}$$

In particular, $\theta_0 \to \varphi_0 + \pi$ and $(x_0, y_0) \to (0,1)$ as $b \to 0$ (note that the length of $\widetilde{v}_2$ goes to zero). This implies that the first component of equation (3.7) is positive – that is, $\gamma(0)$ and $\gamma(\pi)$ lie at distinct sides of the y-axis for b small enough – so γ intersects the positive y-axis at some point. By Lemma 5, if $a \in (0, a_{\max}(\varphi_0))$ tends to zero, then $b = f(a, \varphi_0)$ also tends to zero and

$$\lim_{a\to 0} \mathcal{P}_2(a, \varphi_0, f(a, \varphi_0)) = \lim_{a\to 0} \left(\frac{x_0 \sin(\theta_0)}{y_0} - \cos(\theta_0) \right) = \cos(\varphi_0).$$

As for the limit $a \to a_{\max}(\varphi_0)$, let $(a_n, \varphi_0) \in \Omega$ be a sequence with $a_n \to a_{\max}(\varphi_0)$. Lemma 5 tells us that $b_n = f(a_n, \varphi_0) \to +\infty$, so the surfaces $\Sigma(a_n, \varphi_0, b_n)$ converge, up to a subsequence and vertical translations (in such a way that h_1 is a segment at height 0) to a solution Σ_∞ of a Jenkins–Serrin problem over an isosceles triangle with values 0 along the unequal side and $+\infty$ and $-\infty$ along the other sides. We will denote in the sequel the elements of $\Sigma(a_n, \varphi_0, b_n)$ with a subindex n.

- If $l < \infty$, the conjugate surfaces converge to $\widetilde{\Sigma}_\infty$, twice the fundamental piece of a symmetric saddle tower with four ends in the quotient (this conjugate construction is analyzed in [16]). If we fix $\widetilde{v}_{2n} \subset \mathbb{H}^2 \times \{0\}$, then the curves $\widetilde{v}_{1n}$ converge to a complete horizontal curve $\widetilde{v}_{1\infty} \subset \mathbb{H}^2 \times \{-l\}$ (convex toward the exterior of the domain), and the curves $\widetilde{h}_{3n}$ tend to an ideal vertical segment $\widetilde{h}_{3\infty}$ (see Figure 6). However, we will translate and rotate the surfaces first so that $\widetilde{v}_{2n}(0) = (0,1,0)$ and $\widetilde{v}'_{2n}(0) = -\partial_x$ in the half-space model in order to analyze the rotation θ_{0n} of $\widetilde{v}'_{2n}$ with respect to the horocycle foliation (i.e., we adapt the sequence to the setting

of Figure 3). This means that a subsequence of $\Sigma(a_n,\varphi_0,b_n)$ converges no longer to a saddle tower but to a subset of the vertical plane $x^2+y^2=1$. Therefore, $\theta_{0n}\to\frac{3\pi}{2}$ and $\widetilde{v}_{2n}(b_n)=(x_{0n},y_{0n})\to(-1,0)$ as $n\to\infty$. In view of equation (3.7), we deduce that γ_n does not intersect the positive y-axis for large n, and equation (3.3) implies that $\mathcal{P}_2(a_n,\varphi_0,b_n)\to+\infty$.

- If $l=\infty$, then it is also well known [16, 20] that the conjugate surfaces converge to $\widetilde{\Sigma}_\infty$, a quarter of a horizontal catenoid when we keep the point $\widetilde{v}_{2n}(b_n)$ fixed (and hence the curves $\widetilde{v}_{1n}$ converge to a complete ideal horizontal geodesic $\widetilde{v}_{1\infty}\subset\mathbb{H}^2\times\{-\infty\}$). However, if we fix $\widetilde{v}_{2n}(0)=(0,1,0)$ and $\widetilde{v}'_{2n}(0)=-\partial_x$ instead, then a subsequence converges to a subset of the vertical plane $x^2+y^2=1$ as in the case $l<\infty$, so we can reason likewise. □

Proof of Theorems 1 and 2. Set $k\geq 3$. For each $\frac{\pi}{k}<\varphi<\frac{\pi}{2}$, Lemma 6 ensures that $\mathcal{P}_2(a,\varphi,f(a,\varphi))$ tends to $\cos(\varphi)$ when $a\to 0$ and to $+\infty$ when $a\to a_{\max}(\varphi)$. Since $\cos(\varphi)<\cos\left(\frac{\pi}{k}\right)$ and $\mathcal{P}_2$ is continuous, there exists some $a_\varphi\in(0,a_{\max}(\varphi))$ such that $\mathcal{P}_2(a_\varphi,\varphi,f(a_\varphi,\varphi))=\cos\left(\frac{\pi}{k}\right)$, though it might not be unique. Therefore, we deduce from Lemma 6(c) that $\widetilde{\Sigma}_\varphi=\widetilde{\Sigma}(a_\varphi,\varphi,f(a_\varphi,\varphi))$ solves both period problems. We will show that $\Sigma_\varphi=\Sigma(a_\varphi,\varphi,f(a_\varphi,\varphi))$, and hence $\widetilde{\Sigma}_\varphi$, has finite total curvature by adapting Collin and Rosenberg's argument [2, Remark 7].

To this end, we consider first the case $l=\infty$. For each $k\in\mathbb{N}$, let $p_1(k)\in\ell_3$ be such that $d(p_1(k),p_3)=k$, and let $\ell_2(k)$ (resp., $\ell_3(k)$) be the geodesic segment joining p_3 and $p_1(k)$ (resp., p_2 and $p_1(k)$). For each $n\in\mathbb{N}$ with $n\geq f(a_\varphi,\varphi)$, we will consider the Dirichlet problem over the triangle of vertices $p_1(k)$, p_2, and p_3 with boundary values $f(a_\varphi,\varphi)$ on ℓ_1, n on $\ell_2(k)$, and 0 over $\ell_3(k)$. These conditions span a unique compact minimal disk $\Sigma_\varphi^{k,n}$ (with boundary), which is a graph over the interior of the triangle. The surface $\Sigma_\varphi^{k,n}$ has geodesic boundary and six internal angles, all of them equal to $\frac{\pi}{2}$, so the Gauss–Bonnet formula gives a total curvature of $-\pi$ for $\Sigma_\varphi^{k,n}$. As $k\to\infty$, the surfaces $\Sigma_\varphi^{k,n}$ converge uniformly on compact subsets (as graphs) to a surface Σ_φ^n over Δ with boundary values $f(a_\varphi,\varphi)$ over ℓ_1, n over ℓ_2, and 0 over ℓ_3 (this convergence is monotonic by the maximum principle). Therefore, Fatou's lemma implies that the total curvature of Σ_φ^n is at least $-\pi$. Finally, we let $n\to\infty$ so the Σ_φ^n converge (also monotonically) to Σ_φ on compact subsets, and the same argument implies that Σ_φ has finite total curvature at least $-\pi$ (note that the Gauss curvature of a minimal surface in $\mathbb{H}^2\times\mathbb{R}$ is nowhere positive, by the Gauss equation). If $l<\infty$, the same idea works by just truncating at height n (i.e., there is no need to introduce the sequence with index k).

By successive mirror symmetries across the planes containing the components of $\partial\widetilde{\Sigma}_\varphi$, we get a complete proper Alexandrov-embedded minimal surface $\overline{\Sigma}_\varphi\subset\mathbb{H}^2\times\mathbb{R}$.

- If $l=\infty$, then the curve $\widetilde{v}_1$ is an ideal horizontal geodesic, and we only need to reflect once about a horizontal plane – that is, the plane containing $\widetilde{v}_2$ and $\widetilde{v}_3$. Hence $\overline{\Sigma}_\varphi$ consists of $4k$ copies of $\widetilde{\Sigma}_\varphi$, so the total curvature in this case is not less than $-4k\pi$, and [5, Theorem 4] ensures that $\overline{\Sigma}_\varphi$ is asymptotic to a certain geodesic polygon at infinity. From the foregoing analysis, each end of $\overline{\Sigma}_\varphi$ has asymptotic boundary consisting of four complete ideal geodesics: two horizontal ones obtained from $\widetilde{v}_1$ and two vertical ones obtained from $\widetilde{h}_2$. Taking into account that $\overline{\Sigma}_\varphi$ has

genus $g = 1$, equation (1.1) (with $m = k$) reveals that its total curvature is exactly $-4k\pi$.

Note that each end of $\overline{\Sigma}_\varphi$ is asymptotic to a vertical plane and is contained in four copies of $\widetilde{\Sigma}_\varphi$. We claim that the subset of $\overline{\Sigma}_\varphi$ formed by these four copies is a symmetric bigraph, so in particular the end is embedded. This claim follows from the fact that two of these four pieces come from Σ_φ and its axially symmetric surface with respect to h_2, which project to a quadrilateral of $\mathbb{H}^2$. Since this quadrilateral is convex, the Krust-type result in [8] guarantees that the conjugate $\widetilde{\Sigma}_\varphi$ and its mirror symmetric surface across $\widetilde{h}_3$ form a graph. The other two copies needed to produce the aforesaid bigraph are their symmetric ones with respect to the slice containing $\widetilde{v}_2$ and $\widetilde{v}_3$.

- If $l < \infty$, then the composition of the reflections with respect to the horizontal planes containing $\widetilde{v}_1$ and $\widetilde{v}_3$ is a vertical translation T of length $2l$. Thus, $\overline{\Sigma}_\varphi$ induces a surface in the quotient of $\mathbb{H}^2 \times \mathbb{R}$ by T with total Gauss curvature at least $-4k\pi$, since it consists of $4k$ pieces isometric to $\widetilde{\Sigma}_\varphi$. This surface has genus 1 and $2k$ ends, so it follows from the main theorem in [4] that its total curvature is exactly $-4k\pi$. This result also implies that each end of $\overline{\Sigma}_\varphi$ is asymptotic to a vertical plane (in the quotient). □

Remark 2. It is important to notice that we have not proved the uniqueness of the surface Σ_φ. This would be automatically true if we could show that the second period $\mathcal{P}_2(a,\varphi,f(a,\varphi))$ is strictly increasing in the parameter a, though a comparison of the surfaces for different values of a seems to be difficult, since we do not even know whether the function f solving the first period problem is monotonic.

As φ approaches $\frac{\pi}{k}$, the value a_φ solving the two period problems in the proof of Theorems 1 and 2 goes to zero, and the surface $\widetilde{\Sigma}_\varphi$ converges, after rescaling, to a genus 1 minimal k-noid in $\mathbb{R}^3$ (as in Lemma 5(b)). Moreover, when φ approaches $\frac{\pi}{2}$, the surface Σ_φ converges to an open subset of a helicoid in $\mathbb{R}^3$ after rescaling, and it follows that the conjugate surfaces $\widetilde{\Sigma}_\varphi$ must converge to a quarter of a catenoid in $\mathbb{R}^3$ (the curve $\widetilde{h}_1$ converges to half of the neck of such a catenoid).

3.3. The embeddedness problem

In the proof of Theorems 1 and 2, it is shown that the conjugate piece $\widetilde{\Sigma}_\varphi$ is a graph over the domain $\widetilde{\Delta} \subset \mathbb{H}^2$. But it could happen that when we reflect $\widetilde{\Sigma}_\varphi$ over the vertical plane containing $\widetilde{h}_1$, the resulting surface is not embedded, since the reflected curve of $\widetilde{v}_3$ might intersect $\widetilde{v}_3$. Observe that as the family of examples with k ends converges to a genus 1 minimal k-noid in $\mathbb{R}^3$ after blowup (see also [13]), there do exist nonembedded examples of k-noids and saddle towers with genus 1 in $\mathbb{H}^2 \times \mathbb{R}$ for all $k \geq 3$.

Therefore, embeddedness is guaranteed if the extended surface by reflection about the vertical plane containing $\widetilde{h}_1$ is embedded. The Krust property yields this if the initial surface Σ_φ extended by axial symmetry about the geodesic h_1 is still a graph over a convex domain – that is, if the angle of Δ at p_3 is at most $\frac{\pi}{2}$. Elementary hyperbolic

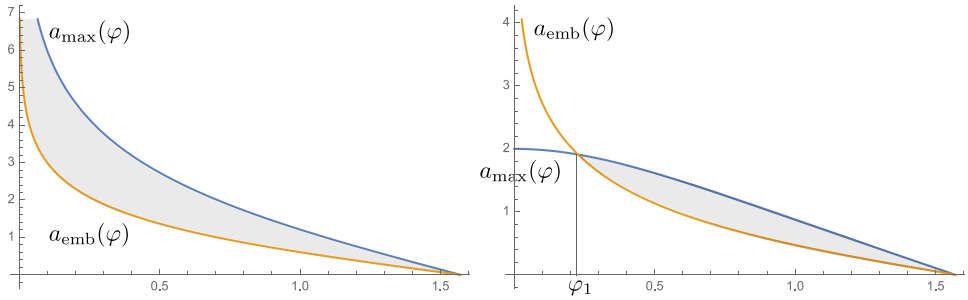

Figure 7. Graphics of the functions $\varphi \mapsto a_{\max}(\varphi)$ and $\varphi \mapsto a_{\mathrm{emb}}(\varphi)$ with $l = \infty$ (left) and $l = 1$ (right). In the shaded regions, embeddedness is guaranteed by the Krust property.

geometry shows that this is equivalent to $a \geq a_{\mathrm{emb}}(\varphi)$, where

$$a_{\mathrm{emb}}(\varphi) = \operatorname{arc\,sinh}(\tanh(l)\cot(\varphi)), \tag{3.9}$$

and $\tanh(l) = 1$ if $l = \infty$. Hence, the surfaces in Theorems 1 and 2 are properly embedded, provided that $a_{\mathrm{emb}}(\varphi) \leq a_\varphi < a_{\max}(\varphi)$. If $l = \infty$, then $a_{\mathrm{emb}}(\varphi) < a_{\max}(\varphi)$ for all $\varphi \in \left(0, \frac{\pi}{2}\right)$; if $l < \infty$, there exists $\varphi_1 \in \left(0, \frac{\pi}{2}\right)$ such that $a_{\mathrm{emb}}(\varphi) < a_{\max}(\varphi)$ if and only if $\varphi \in \left(\varphi_1, \frac{\pi}{2}\right)$ (see Figure 7).

However, on the one hand it seems difficult to know whether a value of a_φ solving both period problems lies in this interval; on the other hand, embeddedness may occur even if $a \geq a_{\mathrm{emb}}(\varphi)$ does not hold. It is expected that there are always values of (a, φ) producing embedded examples solving the two period problems for all $k \geq 3$, and it seems reasonable that this occurs when φ becomes close to $\frac{\pi}{2}$.

3.4. Examples with infinitely many ends

Let us tackle the proof of Theorem 3, which is a particular case of the foregoing constructions for $l = \infty$ (the proof can be easily adapted to the case $l < \infty$). Lemma 6 and the continuity of $\mathcal{P}_2$ imply that for all $\varphi \in \left(0, \frac{\pi}{2}\right)$, there are values of $a \in (0, a_{\max}(\varphi))$ such that $\mathcal{P}_2(a, \varphi, f(a, \varphi))$ is either equal to 1 or greater than 1. Let us study these two cases:

- If $\mathcal{P}_2(a, \varphi, f(a, \varphi)) = 1$, then $\widetilde{h}_1$ and $\widetilde{h}_3$ are contained in vertical planes over asymptotic geodesics of $\mathbb{H}^2$ in view of Lemma 6(d). This means that $\widetilde{\Sigma}(a, \varphi, f(a, \varphi))$ is contained in the region between these two geodesics – see Figure 8 (center) – and mirror symmetries across the corresponding vertical planes span a group of isometries fixing the common point at infinity. This group contains a discrete group of parabolic translations, and gives rise to the 1-parameter family of parabolic ∞-noids.
- The case $\mathcal{P}_2(a, \varphi, f(a, \varphi)) > 1$ occurs in an open subset of Ω, and gives rise to the 2-parameter family of hyperbolic ∞-noids. The two geodesics of $\mathbb{H}^2$ containing the projections of $\widetilde{h}_1$ and $\widetilde{h}_3$ do not intersect in this case, and successive reflections

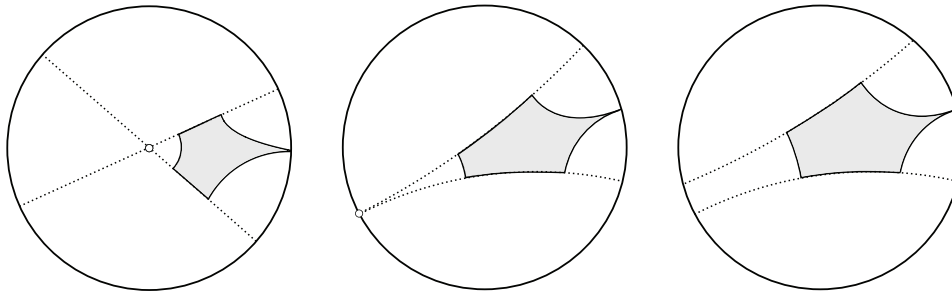

Figure 8. The fundamental domains of a 3-noid (left), a parabolic ∞-noid (middle), and a hyperbolic ∞-noid (right). Dotted curves represent geodesics containing the projection of $\widetilde{h}_1$ and $\widetilde{h}_3$.

across their associated vertical planes span a group of isometries containing a discrete group of hyperbolic translations – see Figure 8 (right).

Similar arguments to those in the proof of Theorems 1 and 2 (using the description of periodic surfaces with finite total curvature in [4]) show that each end of the constructed surfaces is embedded and has finite total curvature, plus the global surface is Alexandrov-embedded. Observe that in the case of hyperbolic ∞-noids, we can always choose $a \geq a_{\text{emb}}(\varphi)$, defined in the previous section, which means that whenever the parameters (a,φ) lie in this open subset of Ω, the reflected surface is a properly embedded hyperbolic ∞-noid . In the case of parabolic ∞-noids, we are not able to guarantee global embeddedness.

Acknowledgments. The authors would like to express their gratitude to Magdalena Rodríguez for her valuable comments during the preparation of this manuscript, as well as to the anonymous referee for the thorough revision of the manuscript, which has greatly improved the final presentation. This research was supported by MINECO–FEDER project MTM2017-89677-P and by MCIN/AEI project PID2019-111531GA-I00. The first author is also supported by the FPU programme from MICINN and by MCIN/AEI project PID2020-117868GB-I00. The second author is also supported by EBM/FEDER UJA 2020 project 1380860.

Competing Interests. The authors declare none.

References

[1] J. Castro-Infantes, J. M. Manzano and M. Rodríguez, A construction of constant mean curvature surfaces in $\mathbb{H}^2 \times \mathbb{R}$ and the Krust property, *Int. Math. Res. Not. IMRN, rnab353*, (2021), https://doi.org/10.1093/imrn/rnab353.

[2] P. Collin and H. Rosenberg Construction of harmonic diffeomorphisms and minimal graphs, *Ann. of Math. (2)* **172**(3) (2010), 1879–1906.

[3] B. Daniel, Isometric immersions into $\mathbb{S}^n \times \mathbb{R}$ and $\mathbb{H}^n \times \mathbb{R}$ and applications to minimal surfaces, *Trans. Amer. Math. Soc.* **361**(12) (2009), 6255–6282.

[4] L. Hauswirth and A. Menezes, On doubly periodic minimal surfaces in $\mathbb{H}^2 \times \mathbb{R}$ with finite total curvature in the quotient space, *Ann. Mat. Pura Appl. (4)* **195**(5) (2016), 1491–1512.

[5] L. Hauswirth, A. Menezes and M. Rodríguez, On the characterization of minimal surfaces with finite total curvature in $\mathbb{H}^2 \times \mathbb{R}$ and $\widetilde{\mathrm{PSL}}_2(\mathbb{R})$, *Calc. Var. Partial Differential Equations* **58**(2) (2019), 80.

[6] L. Hauswirth, B. Nelli, R. Sa Earp and E. Toubiana, Minimal ends in $\mathbb{H}^2 \times \mathbb{R}$ with finite total curvature and a Schoen type theorem, *Adv. Math.* **274** (2015), 199–240.

[7] L. Hauswirth and H. Rosenberg, Minimal surfaces of finite total curvature in $\mathbb{H}^2 \times \mathbb{R}$, *Mat. Contemp.* **31** (2006), 65–80.

[8] L. Hauswirth, R. Sa Earp and E. Toubiana, Associate and conjugate minimal immersions in $M \times \mathbb{R}$, *Tohoku Math. J.* **60** (2008), 267–286.

[9] J. M. Manzano, J. Plehnert and F. Torralbo, Compact embedded minimal surfaces in $\mathbb{S}^2 \times \mathbb{S}^1$, *Comm. Anal. Geom.* **24**(2) (2016), 409–429.

[10] J. M. Manzano and F. Torralbo, New examples of constant mean curvature surfaces in $\mathbb{S}^2 \times \mathbb{R}$ and $\mathbb{H}^2 \times \mathbb{R}$, *Michigan Math. J.* **63**(4) (2014), 701–723.

[11] J. M. Manzano and F. Torralbo, Compact embedded surfaces with constant mean curvature in $\mathbb{S}^2 \times \mathbb{R}$, *Amer. J. Math.* **142**(4) (2020), 1981–1994.

[12] F. Martín, R. Mazzeo and M. Rodríguez, Minimal surfaces with positive genus and finite total curvature in $\mathbb{H}^2 \times \mathbb{R}$, *Geom. Topol.* **18** (2014), 141–177.

[13] L. Mazet, The Plateau problem at infinity for horizontal ends and genus 1, *Indiana Univ. Math. J.* **55**(1) (2006), 15–64.

[14] L. Mazet, M. Rodríguez and H. Rosenberg, The Dirichlet problem for the minimal surface equation –with possible infinite boundary data– over domains in a Riemannian surface, *Proc. Lond. Math. Soc. (3)* **102**(3) (2011), 985–1023.

[15] L. Mazet, M. Rodríguez and H. Rosenberg, Periodic constant mean curvature surfaces in $\mathbb{H}^2 \times \mathbb{R}$, *Asian J. Math.* **18**(5) (2014), 829–858.

[16] F. Morabito and M. Rodríguez, Saddle towers and minimal k-noids in $\mathbb{H}^2 \times \mathbb{R}$, *J. Inst. Math. Jussieu* **11**(2) (2012), 333–349.

[17] B. Nelli and H. Rosenberg, Minimal surfaces in $\mathbb{H}^2 \times \mathbb{R}$, *Bull. Braz. Math. Soc. (N.S.)* **33**(2) (2002), 263–292.

[18] J. Plehnert, Constant mean curvature k-noids in homogeneous manifolds, *Illinois J. Math.* **58**(1) (2014), 233–249.

[19] J. Plehnert, Surfaces with constant mean curvature $\frac{1}{2}$ and genus one in $\mathbb{H}^2 \times \mathbb{R}$, Preprint, 2012, arXiv:1212.2796.

[20] J. Pyo, New complete embedded minimal surfaces in $\mathbb{H}^2 \times \mathbb{R}$, *Ann. Global Anal. Geom.* **40**(2) (2011), 167–176.

[21] J. Pyo and M. Rodríguez, Simply connected minimal surfaces with finite total curvature in $\mathbb{H}^2 \times \mathbb{R}$, *Int. Math. Res. Not. IMRN* **2014**(11) (2014), 2944–2954.